Colours with achromatic materials

L. Simonot, Université de Poitiers, Laboratoire de Physique des Matériaux, UMR 6630 CNRS

We consider very simple structures – only one layer on a substrate – that present saturated colours although they are constituted by achromatic materials: a dielectric (by instance TiO_2) or/and a metal (for instance Ag). A transparent SiO_2 glass sheet is taken for the substrate in order to simulate both reflection and transmission spectra. Since we focus on colour, the spectral range is limited to the visible range [380-780] nm. We present the colorimetric variations in the CIELab space (cf. Appendix) where the colour can be described by its lightness L*, its chroma C* and its hue h*. When the chroma is less than a few units, the colour is achromatic. When the chroma is greater than 10 or 20 units, the colour is saturated.

We limit our presentation to non-scattering materials; we suppose that the heterogeneities in volume (particle dimensions) or in surface (roughness) are strongly smaller than the light wavelength. Hence, light beams are straight and refracted and reflected in the specular directions (given by Snell's laws) at plane effective interfaces. We further assume that the layer is isotropic. Therefore, the optical behaviour difference between both light polarisations is only due to the partial polarisation by reflection at each interface.

Nonetheless, such simple optical structures present surprising colorimetric behaviours in particular the colour inversion at grazing incident angles for the polarisation parallel to the incident plane as detailed below.

A. Achromatic bulk optical properties

In optics, materials are characterized by their complex refractive index $n(\lambda)+ik(\lambda)$ depending on the wavelength λ. We recall that air has a real refractive index constant and equal to 1. We can distinguish two very different classes of optical behaviours: the dielectric and the metallic ones.

1. Achromatic dielectric materials

The dielectric material complex refractive indices are described by Lorentz model that takes into account the oscillations of electrons related to the atom core. In the visible range for most of dielectric materials, the indices can be approximated by Cauchy law:

$$n(\lambda) = n_0 + \frac{A}{\lambda^2}$$
$$k(\lambda) = 0$$

where $n_0>1$ and $A>O$ are constants. A dielectric material is then non absorbent ($k=0$) in the visible range and its real part weakly decreases with the wavelength as observed in figure 1. This is sufficient to explain the dispersion of white light by an interface between air and a dielectric material. The light dispersion by a prism is used in some spectrophotometers and the light dispersion by a water droplet can explain the formation of rainbows. But it does not occur in our case for a dielectric layer because the light dispersion at an interface is recomposed at the second interface parallel to the first one. Finally the small decrease of the refractive index has no real influence in the colouration phenomena presented in the following parts of this paper.

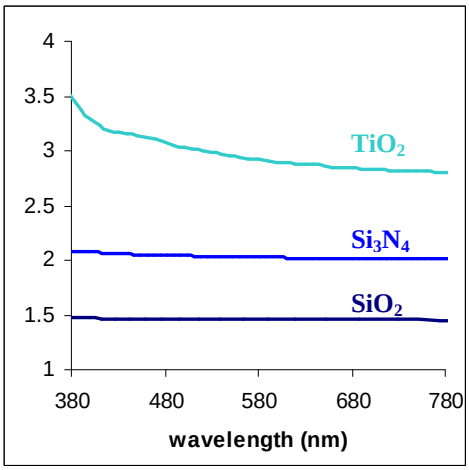

Figure 1: Real refractive index *n* in the visible range for SiO_2, Si_3N_4 and TiO_2

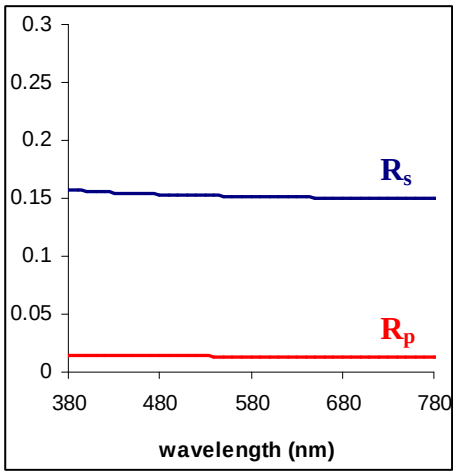

Figure 2: Spectral variation in the visible range for a SiO_2 thick layer in reflection at 45°. Parallel (R_p) and perpendicular (R_s) polarisations

The bulk dielectric material reflectance is the reflectance by an interface between air and the dielectric material. Practically, as the dielectric material is transparent, it would be easier to measure the reflectance of a dielectric layer surrounding by air downwards and upwards. As the material is non absorbent, this reflectance is theoretically independent of its thickness. However, the layer has to be thick enough in order to consider the multiple incoherent emerging rays and therefore not to take into account the interferences. In this way, we can calculate the reflectance of a SiO_2 layer by using the Fresnel relations at each interface whatever the polarisation state. Figure 2 shows the reflection spectra R_s and R_p at 45° for the polarisation respectively perpendicular and parallel to the incidence plane. These reflectances are almost wavelength independent (as observed in every-day life with glass window for instance). Consequently, the chroma calculated from the spectrum is very small (C*<1 whatever the incident angle): the colour is effectively achromatic. The pertinent colorimetric parameter is then the lightness L*. Figure 3 shows the angular variation of L*. At 0°, the lightness of both polarisations are equal and rather small (L*=31). They reach unity for grazing angles. For perpendicular polarisation R_s, the lightness increases monotonously. On the contrary, for parallel polarisation R_p, the lightness passes through a minimum, almost equal to zero, at the Brewster angle θ_B:

$$\theta_B = \tan^{-1}(n)$$
$$\theta_B \approx 55° \qquad \text{for } n_{SiO_2} = 1.45$$

2. Achromatic metallic materials

The metallic materials indices are described by Drude model where the electrons are no more bound to the atomic core but free to move into the metallic crystal. In the visible range, the complex refractive index can be approximated by:

$$\begin{cases} n(\lambda) \approx 1 - \alpha\lambda^2 \\ \kappa(\lambda) \approx \beta\lambda^3 \end{cases}$$

where α and β>O are constants. A metallic material is very absorbent, the imaginary part increasing with the wavelength. The real part is inferior to 1 and weakly decreases with the

wavelength. These properties can be seen in figure 4 with the silver complex refractive index in the visible range. For noble metals (Ag, Au, Cu), the electronic interband transitions has to be added to Drude model. The interband transition has an impact for wavelengths inferior to a wavelength threshold. This threshold is in the visible range for gold and copper: this effect explains the coloured reflections of these metals. For silver, the wavelength threshold is located in the UV range (see figure 4) and this metal is achromatic.

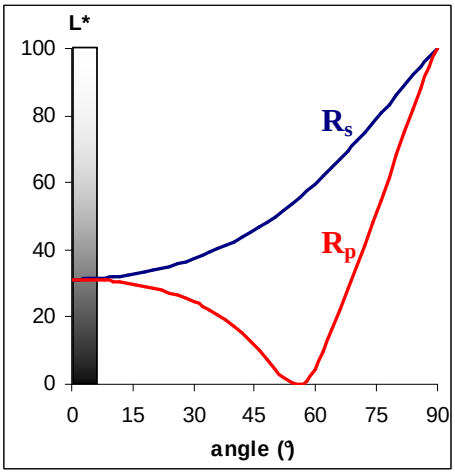

Figure 3: Angular variation of the lightness L* of a SiO_2 thick layer in reflection (the chroma C* is less than 1 unit). Parallel (R_p) and perpendicular (R_s) polarisations

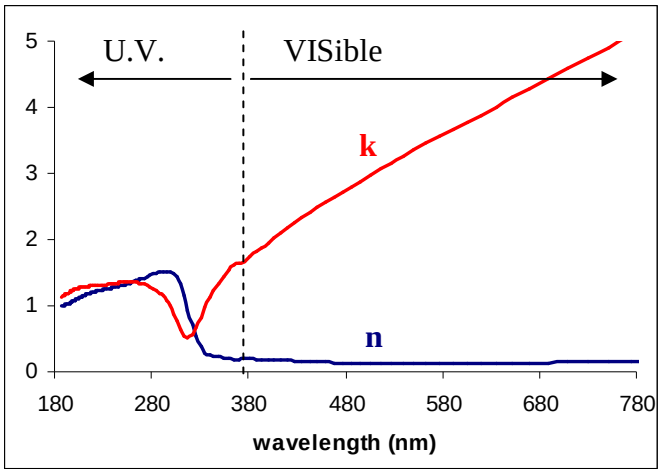

Figure 4: Spectral variations of the Ag refractive index. Real part *n* and imaginary part *k*.

The bulk metallic material reflectance can be calculated from the complex refractive index. As the material is strongly absorbent, the reflectance is rather high. As seen in figure 5, the silver reflectance is almost wavelength independent. Consequently the chroma calculated from the spectrum is rather small (the chroma C* is less than 4 units): the colour is effectively achromatic. The pertinent colorimetric parameter is then the lightness L*. Figure 6 shows the angular variation of L*. Contrary to the dielectric materials, the lightness is high whatever the incident angle. Even if we can define a Brewster angle (around 80°), the difference between both polarisations is weak.

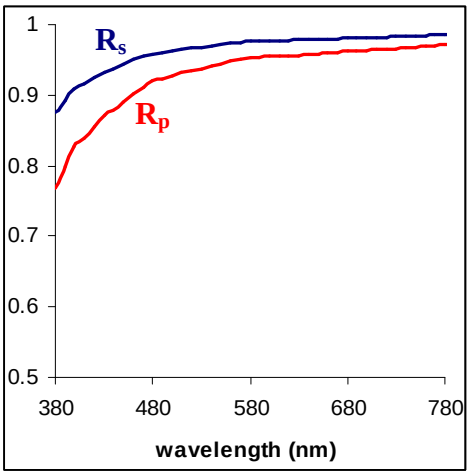

Figure 5: Spectral variation in the visible range of Ag bulk in reflection at 45°. Parallel (R_p) and perpendicular (R_s) polarisations

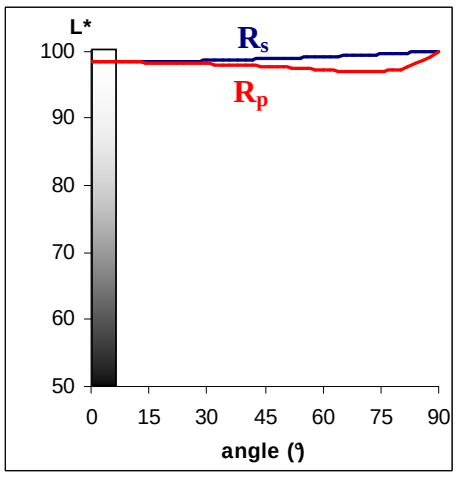

Figure 6: Angular variation of the lightness L* of Ag bulk in reflection (the chroma C* is less than 4 units). Parallel (R_p) and perpendicular (R_s) polarisations

B. Interferential dielectric layer

A first solution to obtain colouration with achromatic materials is to create interferences with a thin dielectric layer. This phenomenon is achieved when the successive emerging rays due to the multiple reflections into the layer are in phase.

We choose the example of a TiO_2 dielectric layer $\left(n_{TiO_2} \approx 3\right)$ on a SiO_2 substrate $\left(n_{SiO_2} \approx 1.45\right)$.

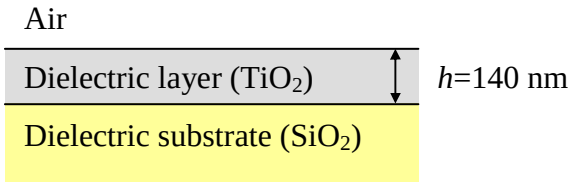

Figure 7: Thin TiO_2 dielectric layer on a SiO_2 substrate

The maxima in transmission are obtained for wavelengths λ that verify:

$$k\lambda = 2n_{TiO_2} h \cos\theta$$

where k is an integer, h the layer thickness and θ the propagating angle inside the layer.

To obtain only one extremum in the visible range, the thickness has to be around 100 to 200 nm. If the layer is thinner, respectively thicker, no extremum, respectively several extrema, are located in the visible range and in both cases, the chroma C* will not be very high.

However, another condition has to be fulfilled: the extremum amplitude has to be important enough. It is possible if the successive emerging rays have similar amplitudes. There has to be a large contrast between the refractive indices at the layer/substrate interface. The chroma is higher with a TiO_2 layer $\left(n_{TiO_2} \approx 3\right)$ on a SiO_2 substrate $\left(n_{SiO_2} \approx 1.45\right)$ than with a Si_3N_4 layer $\left(n_{Si_3N_4} \approx 2\right)$ on the same substrate.

The reflection and transmission spectra $R(\lambda)$ and $T(\lambda)$ can be calculated using the Fresnel relations at each interfaces and the phase relation between the emerging rays (for more details concerning these calculations, see Azzam[1]). As the dielectric materials are non absorbent, the flux balance can be written as: $R(\lambda)+T(\lambda)=1$. Therefore, a minimum in the transmission spectrum is a maximum in the reflection spectrum (see figure 8 for both polarisations with a 45° (left) and 80° (right) incident angle). This property implies that the colours obtained in reflection (green (a*<0) / yellow (b*>0)) are almost the complementary colours of those obtained in transmission (red (a*>0) / blue (b*<0)). Figure 9 presents the colorimetric variations in terms of the incident angle in reflection (figure 9(a)) and in transmission (figure 9(b)) for (chroma C* / lightness L*) plane (left) and for the chromatic (a* / b*) plane (right). It is obvious that high chroma colours (C* greater than 20) are obtained for a large range of incident angles.

The optical behaviour is different between both polarisations in particular for grazing angles. The most surprising phenomenon is the radical colour change for the polarisation parallel to the incident plane (see figure 9) after passing through a roughly achromatic colour for a 72° incident angle. The spectral reflectance maximum for R_p at 45° (near 520 nm) becomes a minimum at 80° (see figure 8). If the Brewster angle is almost wavelength independent for bulk achromatic material (part A), the Brewster angle (annulation of R_p) is strongly wavelength dependent for an interferential layer: it is the reason for this striking effect.

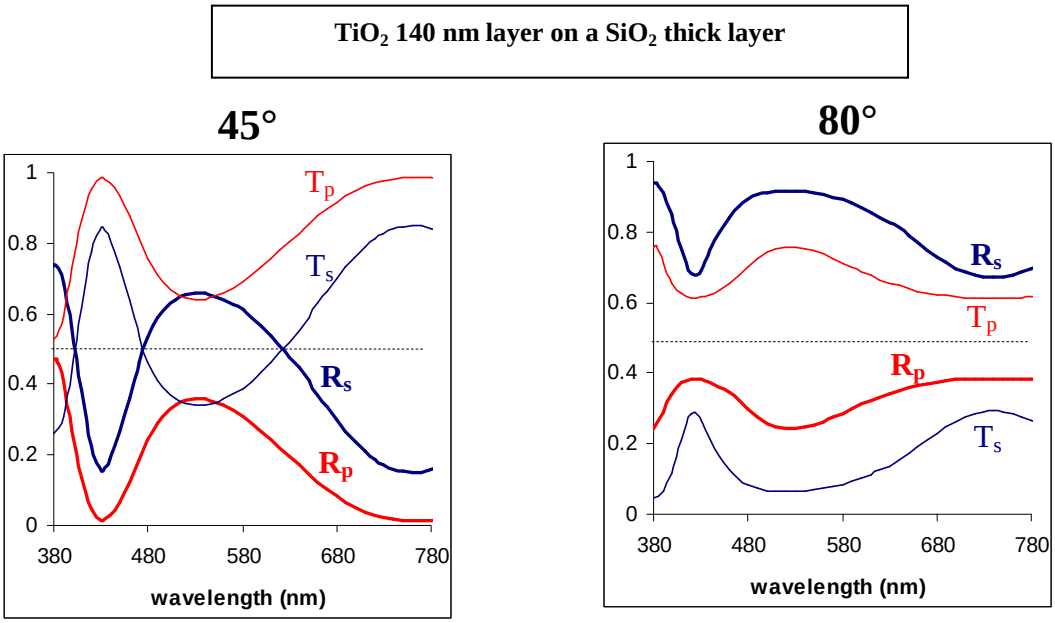

Figure 8: Spectral variation in reflection (R_p, R_s) and in transmission (T_p, T_s).
Incident angle: 45° (left) and 80° (right).

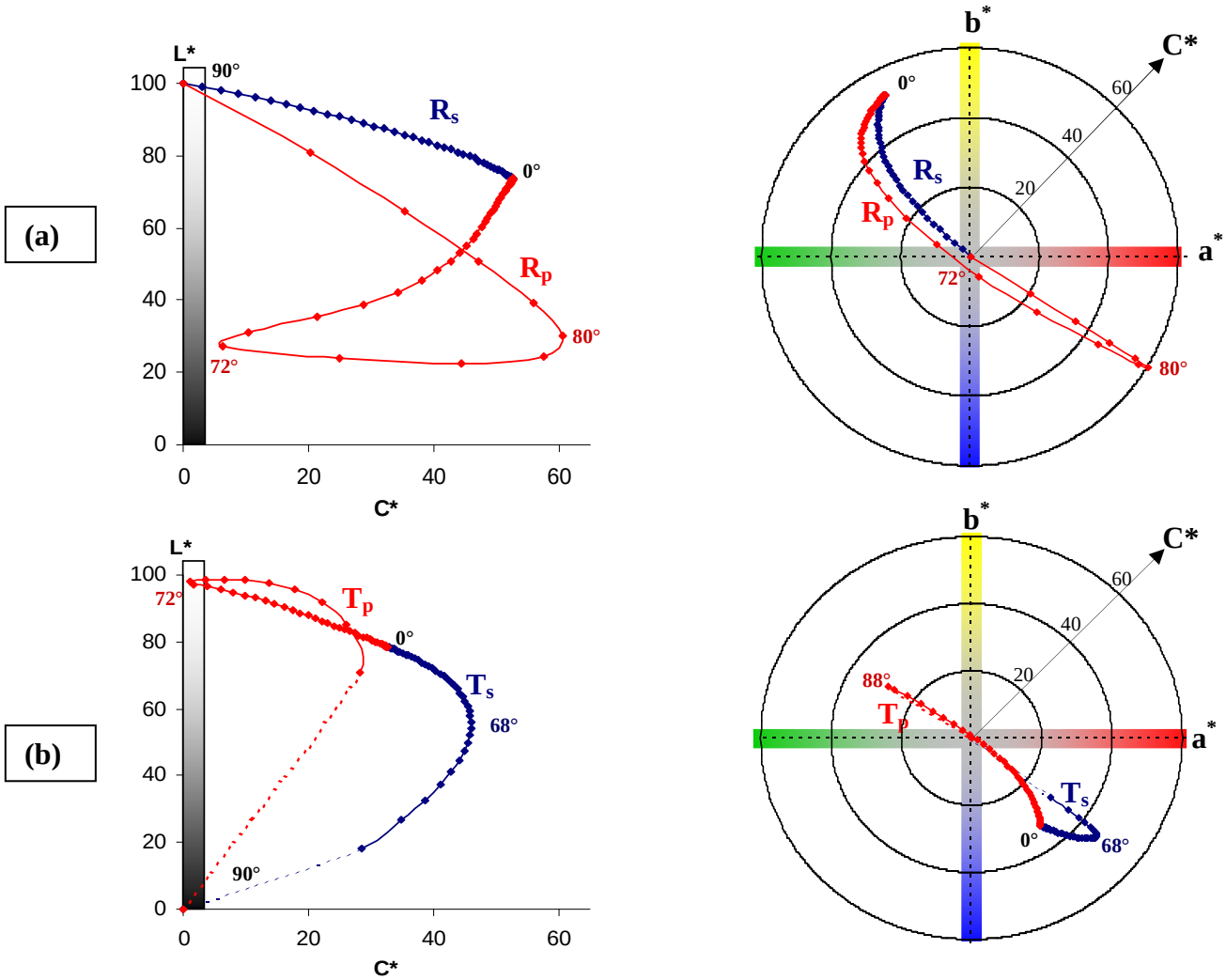

Figure 9: Colorimetric variation in terms of the incident angle (angular step: 2°)
(a) in reflection (R_p, R_s) (b) in transmission (T_p, T_s)

- **for (chroma C* / lightness L*) plane (left)**
- **for the chromatic (a* / b*) plane (right)**

C. Thin layer of metallic aggregates dispersed into a dielectric matrix

It is not possible to have interferential layers with metals because of their absorption. A 60 nm thickness is enough to obtain a layer of silver opaque to visible radiations. The optical behaviour of such layer is then similar to the silver bulk behaviour described in part A.2.

If smaller amount of silver is deposited on a substrate by physical process (ion-beam sputtering, magnetron cathodic sputtering, electron-beam evaporation), a continuous layer does not grow, instead isolated islands do (Volmer-Weber growth mode). The metallic dots are called nanoclusters.

Noble metal nanoclusters exhibit a surface plasmon resonance which induces absorption of light at wavelength generally located in the visible range. The metallic nanoclusters can be incorporated within a dielectric matrix in order to form composite materials called nanocermets. The absorption band depends on the complex refractive indices of both the metallic nanoclusters and the dielectric matrix, on the concentration, sizes, forms and arrangements of the nanoparticles (see references[2-4] with practical examples of silver nanoparticles embedded in different dielectric matrices and deposited on different substrates).

This absorption property of nanocermets can be used to obtain colouration with only achromatic bulk materials. We use here the model of Maxwell-Garnell to simulate the complex refractive index of identical, spherical silver nanoparticles randomly distributed in a dielectric Si_3N_4 matrix. The volume concentration of metallic nanoparticles is assumed to be 10%. Figure 10 shows *n* and *k* obtained with these assumptions.

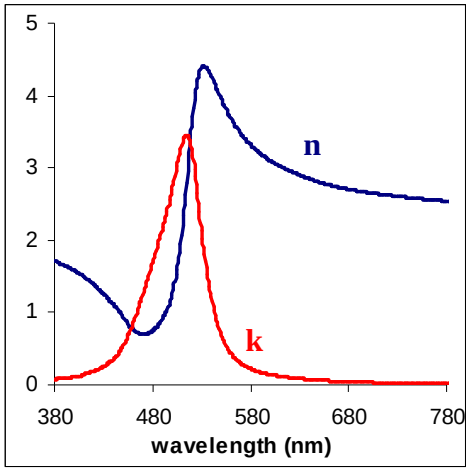

Figure 10: Spectral variations of the effective medium Ag/Si3N4 refractive index obtained by Maxwell-Garnett. Silver volume concentration: 10%. Real part *n* and imaginary part *k*.

Next, we consider a 12 nm layer of such nanocermets as presented in figure 11. As the particle sizes are strongly smaller than the wavelength, there is equivalence with a homogeneous effective medium layer which refractive index is shown in figure 10. Moreover, as we assume spherical particles and random particle dispersion, this effective medium can be considered as isotropic.

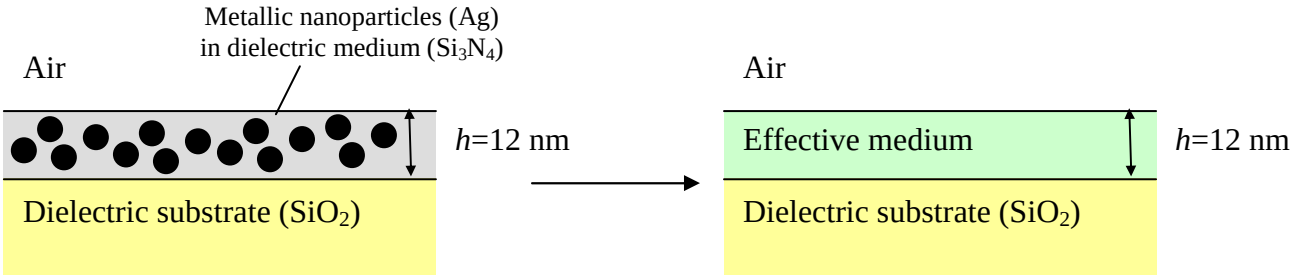

Figure 11: Silver nanoparticles dispersed in a Si_3N_4 matrix on a SiO_2 substrate. Equivalence with an effective medium layer.

The absorption band of these nanocermets is located at 500 nm, the maximum of the refractive index imaginary part (figure 10). Consequently, the transmission (respectively reflection) presents a minimum (respectively maximum) near this wavelength (at 520 nm figure 12 on the left for a 45° incident angle).

Figure 13 presents the colorimetric variations in terms of the incident angle in reflection (figure 13(a)) and in transmission (figure 13(b)) for (chroma C* / lightness L*) plane (left) and for the chromatic (a* / b*) plane (right). It is obvious that high chroma colours (C* greater than 20) are obtained for a large range of incident angles.

We can compare the optical behaviour of an interferential dielectric layer (part B) and of a nanocermet layer (part C). This last one is an absorbing layer, therefore:

- The flux balance can be written as $R(\lambda)+T(\lambda)<1$ contrary to an interferential layer.

  Nevertheless the colours obtained in transmission and in reflection are relatively complementary colours (see figure 13 (a) and (b)).
- The extremum wavelength is almost independent on the incident angle. Therefore, the hue angle is less dependent on the incident angle than for an interferential layer, especially for the polarisation perpendicular to the incident plane (compare R_s colour in figure 9(a) and 13(a) on the right)
- For comparable chroma, the effective medium layer is much thinner than the interferential layer (12 nm compared to 140 nm in the presented examples).

The two last points are crucial advantages in favour of a nanocermet layer for coloured optical filter applications.

A common point between both layers is the colour inversion observed at grazing angles for the polarisation parallel to the incident plane: the Brewster angle in both cases is strongly dependent on the wavelength. For instance, the spectral reflectance maximum for R_p at 45° (near 520 nm) becomes a minimum at 80° (see figure 8). But contrary to an interferential layer, the spectral transmittance minimum for T_p at 45° (near 520 nm) is always a minimum for a 80° incident angle and a second minimum appears at 460 nm (see figure 8). This phenomenon is also due to the Brewster angle. Weak (55°) for 460 nm where the module of the refractive index is minimal, the Brewster angle is much larger (80°) for 520 nm where the module of the refractive index is maximal (see figure 10).

Effective medium 12 nm layer on a SiO_2 thick layer
Maxwell-Garnett : Ag (10%) / Si_3N_4

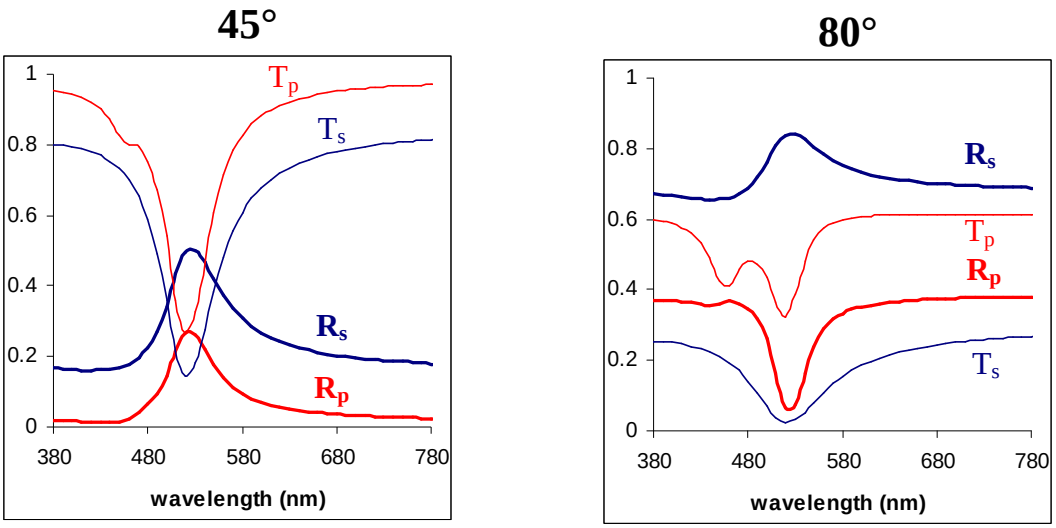

Figure 12: Spectral variation in reflection (R_p, R_s) and in transmission (T_p, T_s).
Incident angle: 45° (left) and 80° (right).

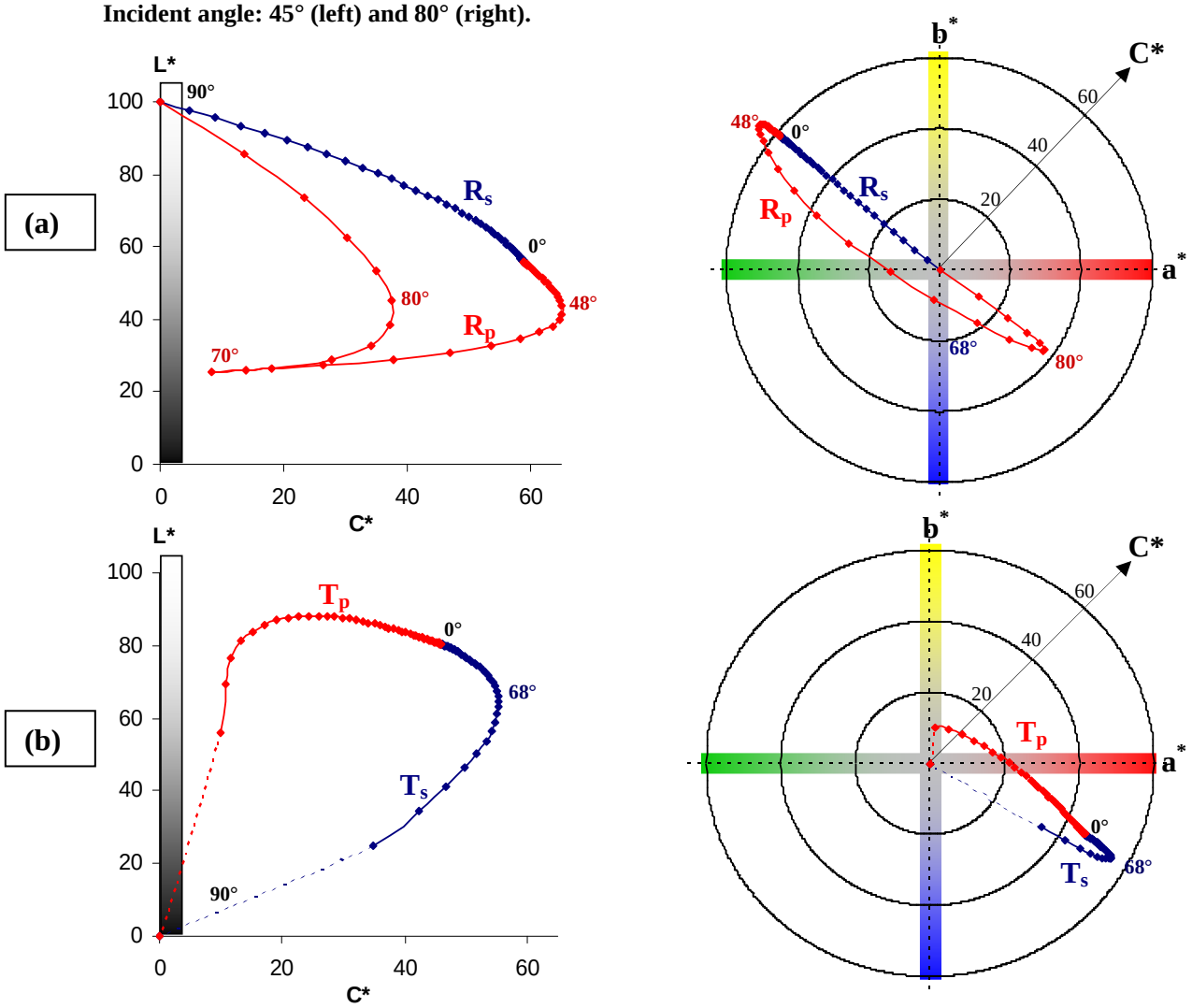

Figure 13: Colorimetric variation in terms of the incident angle (angular step: 2°)
(a) in reflection (R_p, R_s) (b) in transmission (T_p, T_s)

- **for (chroma C* / lightness L*) plane (left)**
- **for the chromatic (a* / b*) plane (right)**

Then, it is possible to obtain saturated colours with achromatic bulk materials with structures at two different scales:

- a submicrometric (around 100 to 200 nm) dielectric layer creating saturated colours by interferences;
- a layer (around severals nm) of nanometric metallic particles creating saturated colours because of surface plasmon resonance inducing an absorption band (in the visible range for noble metals).

We presented simple examples: only one isotropic layer on a transparent substrate. A lot of more complex systems can be proposed to tailor the colour: dielectric multilayer or 2D or 3D nanoparticle organisations with different particles sizes and forms.

In spite of some differences presented above, an interferential layer and an effective medium layer exhibit the same following colorimetric properties:

- a high chroma obtained for a large range of incident angles;
- a dissociation between the reflected and transmitted colours which are almost complementary;
- a clear colour inversion at grazing incident angles for the polarisation parallel to the incident plane.

Appendix: CIELab colourimetric co-ordinates

For more details on colorimetric calculations, see Wyszecki[5]. Photometry and colorimetric are normalized by the CIE, Commission international de l'éclairage.

The CIEXYZ components to define the colour of an object are calculated by taking into account the luminance of a standardised illuminant, the three colorimetric functions related to the retinal cone sensibility and the reflection (or transmission) spectrum of this object. Here, the illuminant D65, which simulates the daylight and the standard observer defined by the CIE in 1931 are chosen.

The CIELab co-ordinates defined by the CIE in 1976 can be deduced from the previous CIEXYZ components. The three CIELab co-ordinates are the achromatic lightness L^* and two chromatic components:

- a^* (green/red axis) and b^* (blue/yellow axis) for the Cartesian co-ordinates;
- chroma $C^* = \sqrt{a^{*2} + b^{*2}}$ and hue angle $h^* = \mathrm{atan}\left(\frac{b^*}{a^*}\right)$ for the polar co-ordinates.

For specular materials, like in this paper, the incident light is used as reference by convention. The CIELab coordinates for the incident light are: L*=100, a*=0, b*=0.

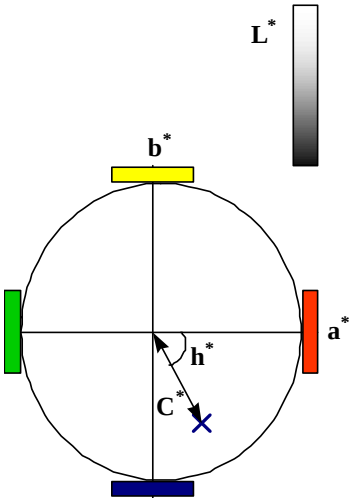

Figure A1: CIELab colorimetric space

References

1. R.M. Azzam, N.M.Bashara, *Ellipsometry and Polarized Light*, North-Holland personal library (1977)
2. J. Toudert, D. Babonneau, L. Simonot, S. Camelio and T. Girardeau, *Quantitative modelling of the surface plasmon resonances of metal nanoclusters sandwiched between dielectric layers: Influence of the nanoclusters size, shape and organization Nanotechnology* **19** (2008) 125709 1-10.
3. S. Camelio, D. Babonneau, D. Lantiat, L. Simonot, *Self-organized growth and optical properties of silver-nanoparticle chains and stripes*, Europhysics Letters **79** (2007) 47002 1-6.
4. S. Camelio, D. Babonneau, T. Girardeau, J. Toudert, F. Lignou, M.F. Denanot, N. Maitre, A. Barranco, P. Guérin, *Optical and structural properties of Ag-Si_3N_4 nanocermets prepared by means of ion-beam sputtering in alternate and codeposition modes***,** Applied Optics **42** (2003), 674-681.
5. G. Wyszecki, WS. Stiles, *Colour science: Concepts and methods, quantitative Data and Formulae*. 2nd ed. Wiley Interscience Publication, New York (1982)